Laminar Flow Control using an Optimised Forward-Facing Step - An Experimental Approach

Chunyi Gao[1,a], Devinder Kumar Yadav[2,b]*, Dinesh Bhatia[3,c]

[1]School of Aerospace University of Nottingham Ningbo China Ningbo, China

[2]School of Aerospace University of Nottingham Ningbo China Ningbo, China

[3]School of Aerospace Engineering University of Glasgow Singapore, Singapore

[a]Email: gaochunyi1999@gmail.com, [c]Email: Dinesh.Bhatia.2@glasgow.ac.uk

[b]*Corresponding author: Email: Devinder.Yadav@nottingham.edu.cn

Abstract - With the rapid increase of global aviation emissions, biomimetics has proven to be a promising avenue to achieve greener aviation. This paper aims to explore the influence of the shark skin denticle inspired two-dimensional Forward-Facing Steps (FFS) on boundary-layer transition delay and drag reduction. Previous computation simulations indicate that the presence of FFS inside the laminar boundary layer can damp disturbances and lead to transition delay and drag reduction. The purpose of this paper is to find the optimal configuration of the FFS through experimental tests and correlate results to previously concluded simulations. Conditional results indicate that the presence of the FFS within the laminar boundary layer is effective in transition delay and drag reduction.

1. INTRODUCTION

Over the past century, greenhouse emissions from aircraft engines have become a critical issue that is detrimental to the environment. In order to minimize the negative effect of aviation related emissions, aircraft drag reduction has been developed by leaps and bounds since the 20th century [1]. However, the conventional methods of drag reduction have plateaued and further advances in drag reduction had levelled off. With the intention of finding new methods of flow control, more experts put their attention into the alternate drag reducing mechanisms like passive flow control [1]. One of the passive flow control methods was the biomimetically inspired Forward-Facing Step (FFS) [1]. A micro scale analysis of the Sharkskin indicates that the sharkskin is composed of many denticles stacked one above the other along the flow direction. The efficiency of shark-skin-inspired geometries has been proved by a sinusoidal surface waves experiment on a flat plate, which resulted in a transition delay of 10.8% and a drag reduction of 5.2% [1] [2]. Therefore, the bionic inspired flow control technique such as Leading-edge serration has been used in practical applications [3].

FFS was a simplified single-step structure based on microscale geometry, which mimicked the shark skin denticles [4]. A 20% transition delay and a 6% drag reduction were achieved in the laminar region based on simulations carried out by Bhatia et al. (2020) [1]. It was found that when the FFS was placed 10% before the transition onset point of the flat plate, the transition delay occurred. By analyzing the Turbulent Kinetic Energy (TKE) contours of different boundary layer to step height (δ/h) values, the

University of Nottingham Ningbo China. *(sponsors)*

critical step height of transition delay was found as δ/h=24 when placed at 40% of the plate length (x/L=0.4) [1].

This paper aims to quantify the influence of shark skin denticles inspired two-dimensional Forward-Facing Steps (FFS) on boundary-layer transition delay and drag reduction through experimental wind tunnel tests [1]. The basic hypothesis of this project is to find the optimal angle of the FFS within the laminar boundary layer which can delay transition and reduce drag. Based on existing literature, a series of controlled trials between a flat plate and different configurations of FFS were carried out using a wind tunnel. Consequently, the aerodynamic forces and surface flow pattern were recorded and analyzed to find the optimal step angle in drag reduction and the possible mechanisms of transition delay.

2.METHODOLOGY AND DATA COLLECTION

2.1.3D model parameter determination

Based on previous research results from Bhatia et al. (2020) [1], it was found that the FFS was effective in drag reduction when it was placed 10% before the transition location. In other words, the FFS was placed at 40% of the flat plate. Therefore, the step location was defined as x/L=0.4. Additionally, the height of the FFS can be defined using the dynamic-similar method with the information from a real shark [5]. Therefore, $5 * 10^{-5}$m high shark skin denticle and the shark swimming speed of 20ms^{-1} were used [6]. By assuming the Reynolds number (Re) of real sharkskin denticle is the same as the FFS in the wind tunnel, the thickness LA of FFS can be calculated as 2mm. In this experiment, a relatively low flow velocity of 20ms^{-1} was selected to obtain a more obvious surface flow pattern phenomenon.

2.2.Modelling process

The modelling process was carried out using 3DExperience software. Based on previous data from Bhatia (2020) and the size limitation of the wind tunnel, the configuration of the flat plate and FFS have been defined in this study (Table 1) [1].

Table 1: 3D model configurations

Configuration	Magnitude
Length	300 mm
Width	304.6 mm
Thickness	7.5 mm
Length of Leading-Edge Curve	72 mm
Height of FFS	2 mm
Location of FFS	120 mm
Diameter of Assembling Hole	6.2 mm

After defining the configurations, the FFS models were shown in figure 1 and 2 below.

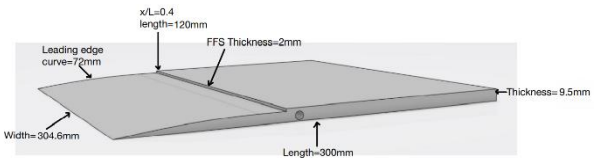

Figure 1. Updated FFS model

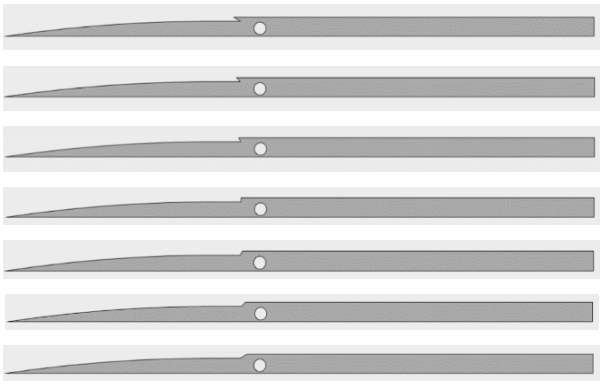

Figure 2. Side view of 30°, 45°, 60°, 90°, 120°, 135°, 150° FFS models

After completing the modelling process, 3D models were printed using resin by 3D printer. Before testing, sandpaper and different types of grinding tools were used to grind the surface of the 3D models to achieve more accurate aerodynamic reaction results and flow patterns.

2.3.Wind tunnel test

Wind tunnel experiments were divided into two aspects known as aerodynamic force measurement and surface flow observation. A subsonic AF-1300 wind tunnel with a three-component balance was used in the experiment as shown in figure 3. Besides, a smoke generator and an ultra-slow-motion camera were used to obtain the surface flow pattern, and basic experimental phenomenon was observed as shown in figure 4. In this experiment, seven typical FFS angles of 30°, 45°, 60°, 90°, 120°, 135°, and 150° were tested. The flat plate model was set as a control group and the flat plates with FFSs on top were set as an experimental group. Subsequently, aerodynamic coefficients and the surface flow pattern for different models were recorded and analyzed.

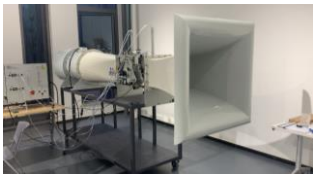

Figure 3. AF-1300 wind tunnel

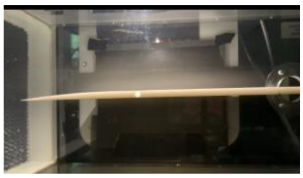

Figure 4. Surface flow pattern of smoke test

2.4.Reliability analysis

To reduce error in the experimental results, the uncertainty analysis was required to be carried out. The uncertainties associated with the measurements of force from 0 to 1.0 N spring scale were calculated. Considering flat plate as an example, the uncertainty associated with drag was calculated as shown below.

$$\delta F = \sqrt{\left(\frac{0.005}{\sqrt{6}}\right)^2 + (0.01 \times F)^2} = \sqrt{\left(\frac{0.005}{\sqrt{6}}\right)^2 + (0.01 \times 1.4)^2} = 1.41\% \quad (1)$$

Where,

$$\delta F \text{ is the uncertainty associated with the force in } N$$
$$F \text{ is the value of force in } N$$

As a result, the average uncertainty of drag for flat plate and FFS models were obtained as 1.06%.

3.RESULTS

The experimental data indicate promising result (Table 2). Subsequently, the drag reduction rate in percentage for different FFS models and flat plate are plotted in this paper (Figure 5).

Table 2: Summary of experimental data

Model	C_D	Drag reduction rate	Transition delay
Flat plate	0.062		/
30°FFS	0.0542	12.6%	/
45 °FFS	0.0360	42.0%	/
60°FFS	0.0462	25.5%	9.8%
90°FFS	0.076	-22.5%	/
120° FFS	0.040	35.4%	/
135° FFS	0.023	62.9%	14%
150° FFS	0.028	54.8%	17%

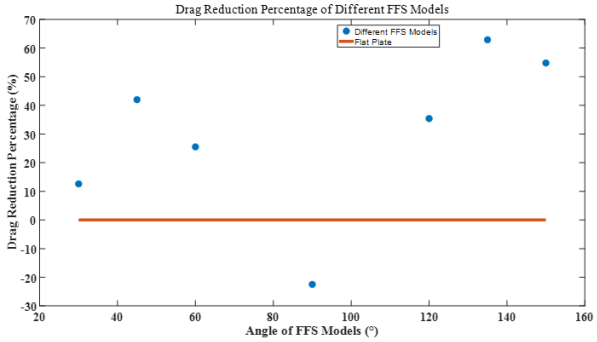

Figure 5. Drag reduction percentage vs. different FFS models and flat plate

According to the results, the optimal angles with positive drag reduction performance were determined as 45°, 135°, 150°, and the drag reduction percentage was 42%, 62.9%, 54.8%, respectively. However, 90° FFS indicated a negative effect on drag reduction performance of -22.5%. The transition delay phenomenon can be observed on the surface of 60°, 135°, and 150° FFS models, which were 9.8%, 14%, 17%, respectively.

4.DISCUSSION

For FFSs from 0° to 90°, the best drag reduction performance occurred at 45° with 42.0% while for 30° and 60° FFS, 12.6% and 25.5% drag reduction are achieved. However, in the range of 09° to 180°, the 135° FFS has the best drag reduction performance with 62.9%. Moreover, 150° FFS can also achieve a high drag reduction percentage of 54.8%. The study shows that the 90° FFS indicates a negative value in drag reduction of minus 22.5%. Therefore, it can be assumed that the overall drag reduction effect of FFS angles within the obtuse angle range is better than that of acute angle range when the FFS is strategically placed at 10% before the transition onset point.

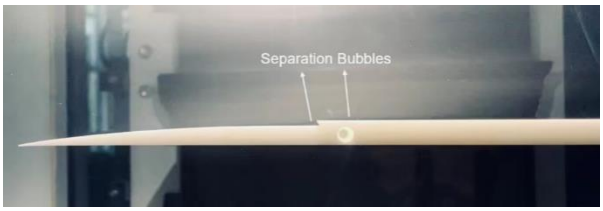

Figure 6. Surface flow pattern of 60° FFS

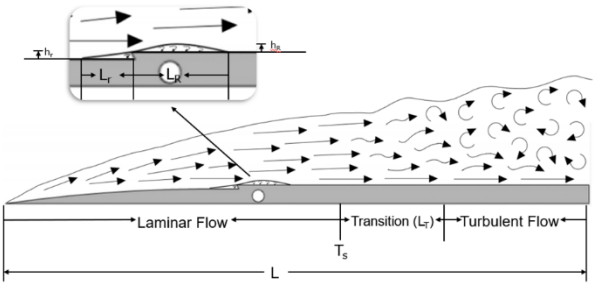

Figure 7. Topological graph of 60° FFS surface flow pattern

Figures 6 and 7 above present the surface flow pattern and topological graph of 60° FFS. According to the streamline pattern of 60° FFS, a small recirculation bubble is formed upstream of the FFS. The length of the upstream separation bubble in front of the step is L_r/L= 0.05 and the height h_r is approximately the same as the step height. Besides, a larger circulation bubble is also formed downstream due to flow separation and reattachment. The length of the downstream separation bubble is certainly larger than that of the small bubble as L_R/L=0.094, and the height h_R/h=1.

Apart from the separation bubbles, there is a redevelopment region after the step, which means the laminar flow on the surface of FFS is not separate at the same location as the flat plate. The flow is energized after the step and the transition starts at T_s/L=0.58, which achieves a 9.8% transition delay compared to the flat plate control group. The length of the transition region is L_T/L=0.19, which is nearly the same as the flat plate. It can also be observed that after the transition region, a vacuum zone was formed and the turbulent vortices in turbulent regions were generated.

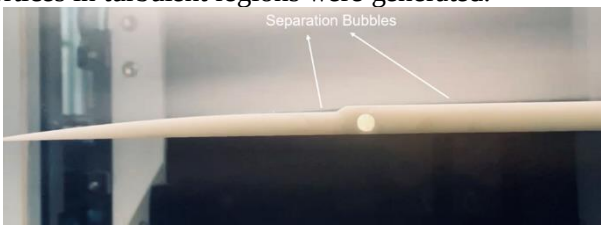

Figure 8. Surface flow pattern of 150° FFS

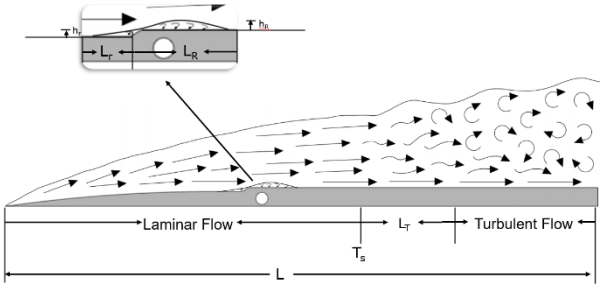

Figure 9. Topological graph of 150° FFS surface flow pattern

As seen from Figures 8 and 9, two separation bubbles are formed due to the presence of the adverse pressure gradient. The length of the upstream separation bubble in front of the step is L_r/L=0.044 while the height hr is the same as the step height of 2 mm. Besides, the length of the downstream separation bubble is L_R/L=1.06, and the height is h_R/h=1.3.

With the increase of the step angle, the downstream separation bubble is further delayed, and the redevelopment region also moves backward on the surface consequently. Similarly, the transition onset point is at T_s/L=0.61, which is delayed 17% compared to the flat plate control group. The length of the transition region is L_T/L=0.18. Likewise, the turbulent flow is formed due to the adverse pressure gradient after the transition region.

Table 3: Parameters of surface flow observation test

Models	L_r/L	h_r/h	L_R/L	h_R/h	T_s/L	Transition delay	L_T/L
Flat plate	/	/	/	/	0.48	/	0.20
60° FFS	0.05	1	0.094	1	0.58	9.8%	0.19
135° FFS	0.044	1	0.105	1.3	0.62	14%	0.19
150° FFS	0.044	1	0.105	1.3	0.61	17%	0.18

The data of flow observation tests are obtained and analyzed (Table 3). With the change of the step angle, the size of the upstream separation bubbles is almost the same while the size of the downstream separation bubbles is different. As mentioned in the table, the height for 135° FFS and 150° FFS downstream separation bubbles are $h_R/h=1.3$, which is bigger than that for 60° FFS of $h_R/h=1$. Likewise, the length for 135° FFS and 150° FFS downstream separation bubbles are $L_R/L=0.105$ that is longer than that for 60° FFS of 0.094. In addition, the transition delay for 60° FFS is 9.8%, which is smaller than 135° FFS and 150° FFS with 14% and 17%, respectively. Therefore, a potential drag reduction mechanism of FFS is such that the transition delay is determined by the downstream separation bubble.

5. CONCLUSIONS

To reduce greenhouse gas emissions and to improve aircraft performance, the sharkskin denticle inspired forward-facing step concept was tested and correlated to simulated results obtained by researchers of this field in the past. Therefore, the effect of step height and step location on transition delay and drag reduction was referenced from the previous research to assist further optimization of FFS configurations. In this paper, a series of wind tunnel experiments were carried out to investigate the effect of different FFS angles on transition delay and drag reduction within the laminar boundary layer.

It was discovered that the 45°, 135°, and 150° FFS have the optimal drag reduction percentage of 42.0%, 62.9%, 54.8%, respectively. Besides, 60°, 135°, and 150° FFS models can delay the transition compared to flat plate model, which were 9.8%, 14%, 17%, respectively. By analyzing the surface flow patterns of different FFS models, it was found that the overall drag reduction performance of FFS angles within the obtuse angle range is better as compared with that of acute angle when the FFS is strategically placed at 10% before the transition onset point. According to the assumption related to the effects of FFS on drag reduction, the length of the FFS downstream separation bubble dictates the transition delay.

ACKNOWLEDGEMENTS

The authors wish to thank the Ningbo Science & Technology Bureau for their funding under the Ningbo Natural Science Programme Project having project code: 2019A610116. The authors would also like to thank the University of Nottingham Ningbo China for their funding under the Faculty of Science and Engineering's New Researcher Grant (NRG).

REFERENCES

[1] D. Bhatia et al., "Laminar Flow Control and Drag Reduction using Biomimetically Inspired Forward Facing Steps," *Journal of Applied and Computational Mechanics,* vol. 7, no. 2, pp. 1-12, 2020, doi: 10.22055/JACM.2020.35082.2557

[2] M. Serdar Genç, K. Koca, H. Demir and H. Hakan Açıkel, "Traditional and New Types of Passive Flow Control Techniques to Pave the Way for High Maneuverability and Low Structural Weight for UAVs and MAVs", 2021.

[3] Z. Wang and M. Zhuang, "Leading-edge serrations for performance improvement on a vertical-axis wind turbine at low tip-speed-ratios", *Applied Energy*, vol. 208, pp. 1184-1197, 2017. Available: 10.1016/j.apenergy.2017.09.034

[4] D. Bhatia, "Biomimetics - A Potential Solution to Drag Reduction in Modern Aerodynamics", *Global Journal of Engineering Sciences,* vol. 3, no. 4, 2019. Available: 10.33552/gjes.2019.03.000568.

[5] K. Gemba, "Measurement of Boundary Layer on a Flat Plate", *Web.iitd.ac.in*, 2007. [Online]. Available: http://web.iitd.ac.in/~pmvs/courses/mel705/boundarylayer.pdf. [Accessed: 08- Nov- 2020].

[6] A. Domel, G. Domel, J. Weaver, M. Saadat, K. Bertoldi and G. Lauder, "Hydrodynamic properties of biomimetic shark skin: effect of denticle size and swimming speed", *Bioinspiration & Biomimetics*, vol. 13, no. 5, p. 056014, 2018. Available: 10.1088/1748-3190/aad418.